Archives of Virology (2018) 163:1043–1049
https://doi.org/10.1007/s00705-018-3704-2

BRIEF REPORT

Mitochondrial bioenergy alterations in avian HD11 macrophages infected with infectious bronchitis virus

Sergio E. L. da Silva[1] · Helena L. Ferreira[2] · Andrea F. Garcia[4] · Felipe E. S. Silva[3] · Roberto Gameiro[3] · Carolina U. F. Fabri[3] · Dielson S. Vieira[3] · Tereza C. Cardoso[3]

Received: 28 August 2017 / Accepted: 22 November 2017 / Published online: 4 January 2018

Abstract

To establish an association between mitochondrial dysfunction and apoptosis following infectious bronchitis virus (IBV) infection, HD11 avian macrophage cells were infected with the Massachusetts 41 (M41) strain. Our results show that the M41 strain of IBV induced cytopathic effects followed by the release of new viral particles. Elevated numbers of apoptotic cells were observed at 24, 48 and 72 h post-infection (p.i.). Viral infection was associated with mitochondrial membrane depolarization and reactive oxygen species (ROS) production at all of the examined timepoints p.i. In summary, IBV M41 replication in infected HD11 macrophages seems to induce mitochondrial bioenergy failure, acting as a respiratory chain uncoupler, without compromising viral replication.

Infectious bronchitis virus (IBV) is taxonomically classified within the order *Nidovirales*, subfamily *Coronavirinae* and genus *Gammacoronavirus* and is associated with respiratory disorders in poultry [2, 5, 8–10, 15]. Macrophages are members of the mononuclear phagocyte system and represent the first line of adaptive immune response by destroying invading pathogens [6, 13]. An important difference between mammalian and avian lungs is the lack of lymph nodes and resident macrophages in the avian respiratory tract, thus requiring an influx of phagocytic cells to initiate the defense against infectious agents [12, 21].

Apoptosis is one of the primary mechanisms that animals use to combat viral infections [11]. By inducing cell death, infected cells and viruses contained within the are eliminated [7, 14]. Apoptosis can be triggered in two ways: intrinsic and extrinsic pathways [11]. Extrinsic pathway activation depends on a variety of external factors, such as cytokines, toxins, or ligands binding to death receptors on the cell surface. The intrinsic apoptosis pathway is triggered by cell stress, and is induced by viral proteins, DNA damage, or oxidative stress, leading to the activation of molecules on the mitochondrial membrane [16–18, 22, 23].

Mitochondria are implicated directly in several host and viral responses [20]. These organelles participate in major early anti-viral immune responses through changes in their metabolism [19]. Viral infection may interfere with mitochondria bioenergetics by affecting cellular respiratory function. Moreover, viral proteins inserted in mitochondrial membranes present anti- and/or pro- apoptotic effects, affecting cell survival/death pathways [22, 23, 25].

The aim of this study was to investigate whether IBV M41 strain-infected avian macrophages (HD11 cell line) show mitochondrial dysfunction at 24, 48 and 72 h post-infection. For this purpose, apoptosis, reactive oxygen species, and mitochondrial membrane depolarization were investigated in these infected cells.

Chemicals were obtained from Sigma-Aldrich (Sigma-Aldrich, St. Louis, MO, USA), Invitrogen (Life Technologies, Carlsbad, CA, USA) and Applied Biosystems (Foster City, CA, USA). All culture dishes and flasks were purchased from BD Falcon (BD Falcon, Bedford, MA, USA) unless otherwise specified. This study used the IBV M41 strain kindly supplied by the Veterinary College of FCAVJ,

Handling Editor: Sheela Ramamoorthy.

✉ Tereza C. Cardoso
tcardoso@fmva.unesp.br

[1] Faculdade de Medicina Veterinária (FAMEV), Universidade Federal Uberlândia (UFU), Uberlândia, MG, Brazil

[2] Department of Veterinary Medicine, FZEA-USP-University of Sao Paulo, Pirassununga, SP, Brazil

[3] College of Veterinary Medicine, UNESP-University of São Paulo State, Araçatuba, SP, Brazil

[4] Centro Universitário Católico Salesiano Auxilium, UniSLESIANO, Araçatuba, SP, Brazil

UNESP, Jaboticabal, SP, Brazil. IBV M41 was propagated in allantoic fluid from chicken-specific, pathogen-free embryos according to rules established for animal care at the Veterinary College, FMVA, UNESP, Araçatuba, SP, Brazil (protocol number 2016/3456). Viral suspensions were titrated by serial 2-fold dilutions and expressed as embryo infectious dose 50% (EID_{50}) [6]. The HD11 cells, an avian macrophage cell line, were purchased from Banco de Células do Rio de Janeiro (BCRJ), Brazil. The susceptibility of HD11 cells to IBV M41 infection was verified by morphological changes (cytopathic effect), cell proliferation assays, virus recovery after CEK (chicken embryo kidney cell) infection and indirect immunofluorescence assays (IFA) at 24, 48 and 72 h p.i.

For IBV M41 infection, HD11 cells were initially co-cultured with CEK cells, prepared according to a standard protocol as described previously [6], and maintained in Dulbecco's Modified Eagle Media (DMEM; Sigma-Aldrich) supplemented with 10% fetal bovine serum (FBS), antibiotics (100 U penicillin and 100 mg streptomycin/ml), and 1.5 mM L-glutamine [11, 14]. IBV M41 strain infection was performed at a multiplicity of infection (MOI) of 1.0 in cell culture medium, and cells were incubated at 41 °C, 5% CO_2, and 95% humidity at a density of 1 x 10^5 cells/cm^2 for HD11 cells and 2 x 10^4 cells/cm^2 for CEK cells. After 6 h, HD11 cells were removed along with the culture supernatant, placed into 6-well plates, and cultured as unique macrophage cultures. Triplicate wells were used for virus or mock infections at 24, 48, and 72 h post-infection (p.i.). Infected and control HD11 cells were visualized under phase-contrast using an Olympus IX 70 microscope (Olympus, Tokyo, Japan) and at least 10 fields were analyzed for each condition. Photographs were taken at 40 x magnification using cell Sens software (Olympus). The numbers of HD11 cells per slide (n = 5) were assessed using an AxioImager® A.1 light microscope connected to an AxioCam®MRc (Carl Zeiss®, Oberkochen, Germany). The images were processed using AxioVision® 4.8 software (Carl Zeiss®).

$TCID_{50}$ titrations were applied to infected and control (mock-infected cells supplemented with culture medium) HD11 cells to measure infective viral particle recovery, as described previously at all p.i. [14]. Cell proliferation analysis was performed using an *in vitro* Toxicology Assay Kit, an MTT (3-(4,5-dimethylthiazol-2-yl)2,5-diphenyltetrazolium bromide)-based assay, following the manufacturer's instructions. IBV M41 infected cells and control cells were prepared for virus immunostaining as described previously [4]. After being fixed with 4% paraformaldehyde, the cells were hydrated for 15 min followed by incubation overnight at 4 °C with the primary antibody, a monoclonal anti-IBV nucleoprotein antibody (no. nAB90926, Abcam, Cambridge, UK) diluted at 1:50. After three washes, antibody binding was visualized by incubating cells with protein A conjugated to FITC (fluorescein isothiocyanate; Sigma-Aldrich), and nuclear staining was performed by incubating cells with 1 mg/ml of DAPI (4′-6-diamino-2-phenylindole; Sigma-Aldrich®) diluted in Fluormount aqueous medium. Images were collected using an AxioImager A.1 light and an ultraviolet (UV) microscope connected to an AxioCamMRc camera (Carl Zeiss, Oberkochen, Germany) and at least 10 fields from each slide (corresponding to p.i. periods) were analyzed. The results for IBV-reactive cells were expressed as percentage IFA positive cells at each time-point p.i.

To evaluate apoptosis and ROS production, the same HD11 culture conditions were used. Flow cytometric analysis of apoptosis/necroptosis and ROS production was performed using an Attune acoustic focusing cytometer system at 24, 48, and 72 h after IBV M41 infection (Applied Biosystems, Foster City, CA, USA). Apoptosis/necroptosis was measured using a double staining method with the Vybrant Apoptosis Assay Kit (Molecular Probes, Life Technologies) and the APO-BrdU TUNEL Assay Kit (Molecular Probes, Life Technologies) according to the manufacturer's instructions. The differentiation of early apoptotic, secondary necrotic, necroptotic, and viable cells was made according to their phenotype: BrdU +/PI− cells were considered early apoptotic, BrdU−/PI+ were considered necroptotic, BrdU+/PI+ were considered secondary necrotic, and BrdU−/PI− were considered viable cells. The results are expressed as Δ % of each cell phenotype. The ROS production was measured using a Fluorometric Intracellular ROS kit (MAK142, Sigma-Aldrich) according to the manufacturer's instructions. Briefly, 1 x 10^6 cells/ml, were centrifuged and the resulting pellet was mixed in 40 µl of ROS detection reagent solution. In parallel, HD11 cells were treated with 1.5 µM of staurosporine (Sigma-Aldrich) for 6 h to induce apoptosis as a positive control. After treatment, IBV was inoculated into cell cultures and monitored at all indicated times p.i. The ROS positive control used was cells exposed to 5% CO_2 for 30 min.

To perform the mitochondrial membrane potential assay, 2 x 10^3 infected or mock infected cells were incubated with 10 µg/ml of JC-1 (5,5′,6,6″-tetrachloro-1,1′,3,3′-tetrathylbenzimidazolyl-carbocyamine iodide; Molecular Probes, Eugene, OR, USA) for 10 min at 37 °C and analyzed by acoustic flow cytometry performed in the dark as described in a previous study [4]. The HD11 cells were also fixed in 4% of paraformaldehyde and documented to visualize JC-1 probe staining. Cell mitochondria were isolated by a modified procedure based on a previously described method [24]. Next, 500 µl each from a HD11 cell suspension of IBV M41 infected or mock infected cells at each indicated time p.i. were placed into 1 ml of isolation buffer containing 0.21 M mannitol, 70 mM sucrose, 1 mM EGTA, 1 mg/ml BSA, and 5 mM HEPES-KOH, pH 7.4 and homogenized gently three times for 15 s at 1-min intervals. The homogenate was then centrifuged at 3,000 x g for 2 min.

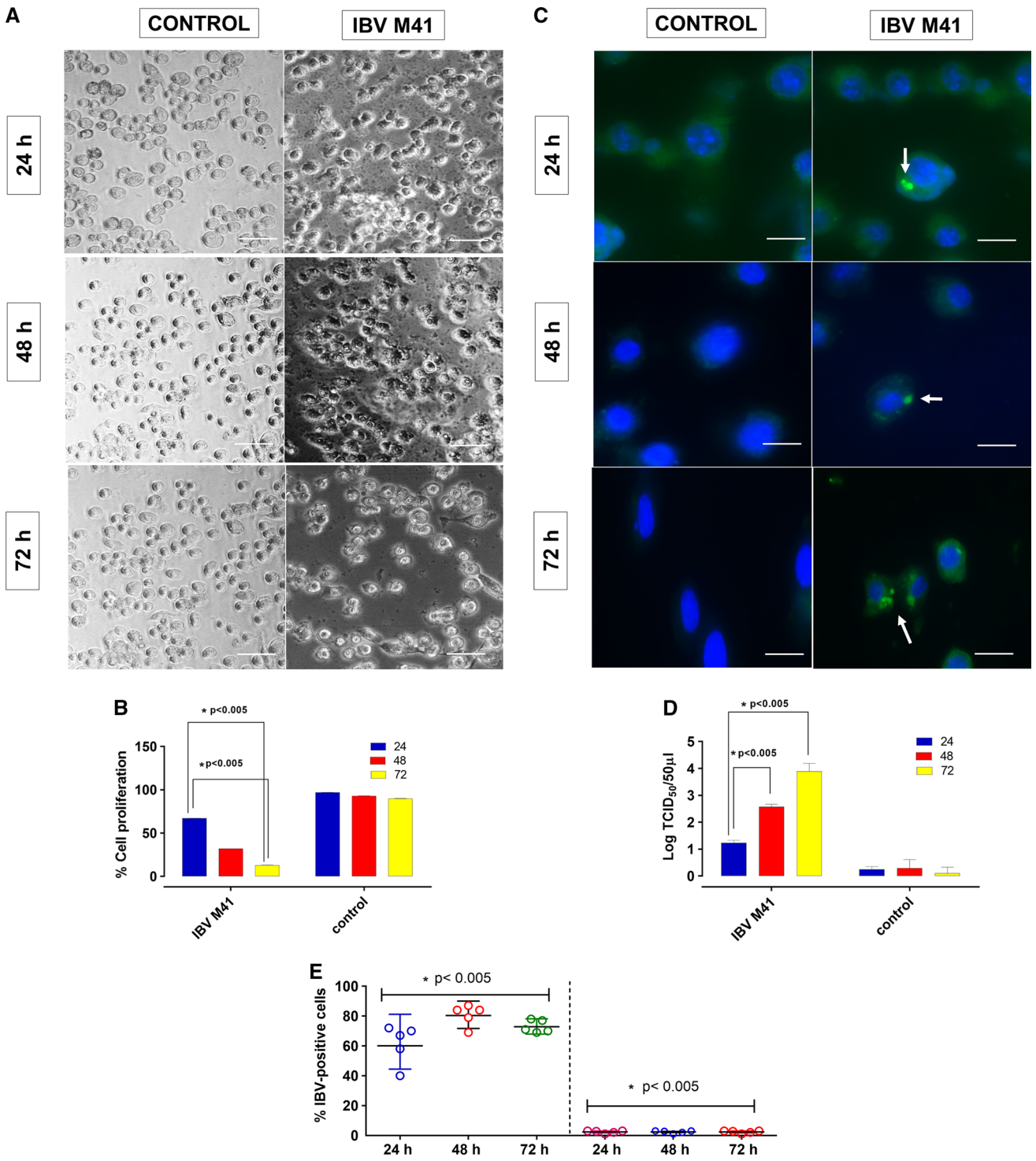

Fig. 1 A) Cytopathic effects in IBV M41 HD11 infected cells at 24, 48, and 72 h p.i. assessed by phase-contrast microscopy. Uninfected HD11 cells were used as controls. IBV M41 cytopathic effects were characterized as lysis and rounding or darkening of cells. Microphotographs are representative of three replicates of each experiment (bars 40-µm). B) Cell proliferation, examined using an MTT assay, indicates progressive decreases, in comparison to uninfected cells (control). C) Analysis of IBV M41 antigen detection (green-arrows) in HD11 cells followed by DAPI counterstaining (blue) by immunocytochemistry at all indicated times p.i. Uninfected HD11 cells (control; bars 40-µm). Microphotographs are representative of three replicates of each experiment. D) IBV M41 titers were calculated to be higher at 72 h p.i. (*$p < 0.005$) and are expressed as CEK $TCID_{50}$. Nascent virus particles were recovered from infected HD11 cells. These data were obtained from three different experiments. E) Frequency of detection of IBV antigen by IFA at 24, 48 and 72 h p.i. The mean value was statistically significant (*p < 0.005) (color figure online)

The resulting supernatant was subsequently centrifuged at 12,000 x g for 20 min. The resulting pellet was suspended in 500 µl of isolation buffer with 0.02% digitonin added and was centrifuged again at 12,000 x g for 10 min. This pellet was then suspended in 1 ml of second buffer containing 0.21 M mannitol, 70 mM sucrose and 5 mM HEPES-KOH, pH 7.4, and centrifuged at 12,000 x g for 10 min. The final pellet was suspended in 250 µl of the second buffer and was used for the respiratory assay. Mitochondria respiration was monitored using a Clark-type oxygen electrode (Strathkelvin Instruments Ltd, Glasgow, Scotland, UK). A total of 1 µg of mitochondrial protein was added to 100 µl of respiration buffer containing 100 mM KCl, 75 mM mannitol, 25 mM sucrose, 5 mM Na_2HPO_4, 0.05 mM EGTA, and 10 mM TRIS-HCI, pH 7.4 at 30 °C. Oxygen consumption was measured using 5 mM succinate (+ 5 nM rotenone) as a respiratory substrate in the absence (state-4 respiration) or presence (state-3 respiration) of 400 nmol ADP. CCCP (m-chlorophenyldrazone) was used at 1 µM as an uncoupler and positive control.

Statistical analysis was performed using GraphPad Instat 6.00 for Windows (GraphPad Software, LaJolla, CA, USA). Three replicates for each experiment were performed, and the results are reported as the mean ± s.d. One-way ANOVA was used for multiple comparisons. Values of $p < 0.05$ were considered to be significant.

The first experiment was conducted to both characterize the replication of the IBV M41 strain in the HD11 cell line and the induced cytopathic effects and release of nascent virus. In this study, a co-culture system of CEK and HD11 cells 6 h after IBV M41 infection was performed to enhance virus replication. The IBV M41 infection was visualized and showed cell lysis and fusiform, 'dark cell' shapes (Fig. 1A). Cell proliferation during IBV M41 replication was evaluated by MTT assay and a progressive loss of cell viability could be detected (Fig 1B). IBV antigen was detected by immunocytochemistry, as indicated by a representative photomicrograph of HD11 cells infected by the IBV M41 strain at 24, 48, and 72 h p.i. (Fig 1C). Thus, a peak viral titer at 72 h p.i., obtained in CEK cells, demonstrated infective IBV particles had been recovered from infected HD11 cells (Fig. 1D). IBV antigens were detected in between 70 and 80% of infected HD11 cells at all time-points p.i. (Fig. 1E). A significant correlation was detected ($r = 0.978$) between virus titer and immunostaining ($p < 0.005$). Interaction of avian viruses and macrophages in culture can be visualized by examining virus-induced cytopathic effects, the presence of viral antigens, and the recovery of new viral particles [21]. While differences in the susceptibility of macrophages to viruses are clearly shown to be dependent upon the source of the macrophages in question, not all avian viruses are able to propagate in macrophage cultures [1, 3, 13, 14]. For example, the HD11 macrophage cell lineage has been shown to be resistant to Marek's disease virus (MDV) and some IBV strains [21]; however, MDV can replicate in macrophages obtained directly from avian organs [3] and Beaudette IBV strain can replicate in HD11 cells [14] whilst IBV M41 can infect the MQ-NCSU culture, as shown recently [1].

To investigate whether apoptosis was occurring during IBV-induced macrophage death, the TUNEL assay was applied at 24, 48, and 72 h p.i. Analysis of IBV-infected HD11 cells revealed early apoptosis which reached the same levels, approximately 65% to 70%, at all timepoints p.i. (Table 1). Similarly, no differences in early apoptosis/necroptosis rates were observed (Table 1). In summary, these results show that IBV M41 strain replication directly affects HD11 viability during an early apoptotic phase. The mitochondrial (intrinsic) pathway is finely regulated, upstream of the organelles themselves, by the concerted action of many molecules, including a family of Bcl-2 proteins, which consists of both pro-apoptotic (BH3-only proteins and multidomain proteins) and anti-apoptotic (Bcl-2-like proteins) members [21]. Several reports describe apoptotic *in vitro* mechanisms related to IBV infection, including both extrinsic and intrinsic pathways [6, 12, 14, 16–18].

IBV M41 infection leads to mitochondria membrane depolarization and ROS production in HD11 cells (Fig. 2 and 3). Moreover, JC-1 probe emission and staining was analyzed (Fig. 2A and B), revealing that the IBV M41 strain produced mitochondrial membrane depolarization at 48 h p.i., which increased at 72 h p.i. (Fig. 2A and B). This finding was confirmed by photomicrographic analysis of JC-1 complexes inside HD11-infected cell cytoplasms (Fig. 2B). Replication of the IBV M41 strain in HD11 cells was able

Table 1 Proportion of BrdU/PI labeled DH11 cells after 24, 48 and 72 h of IBV M41 strain infection

	Dead (% ± sd) (BrdU-/PI+)	Secondary necrotic (% ± sd) (BrdU+/PI+)	Early apoptotic (% ± sd) (BrdU++/PI-)	Viable (% ± sd) (BrdU-/PI-)
24 h	12.7 ± 3.8	9 ± 1.0	67.6 ± 6.0	10.7 ± 1.3
48 h	10 ± 1.5	11.3 ± 2.9	65.8 ± 4.7	12.9 ± 3.6
72 h	16.8 ± 4.9	9 ± 0.9	70.4 ± 3.9	3.8 ± 7.9
Control	5.6 ± 1.2	0.5 ± 0.1	5.0 ± 0.6	88.9 ± 7.8
Staurosporine	70 ± 9.7	16 ± 2.3	10.7 ± 2.7	3.3 ± 1.7

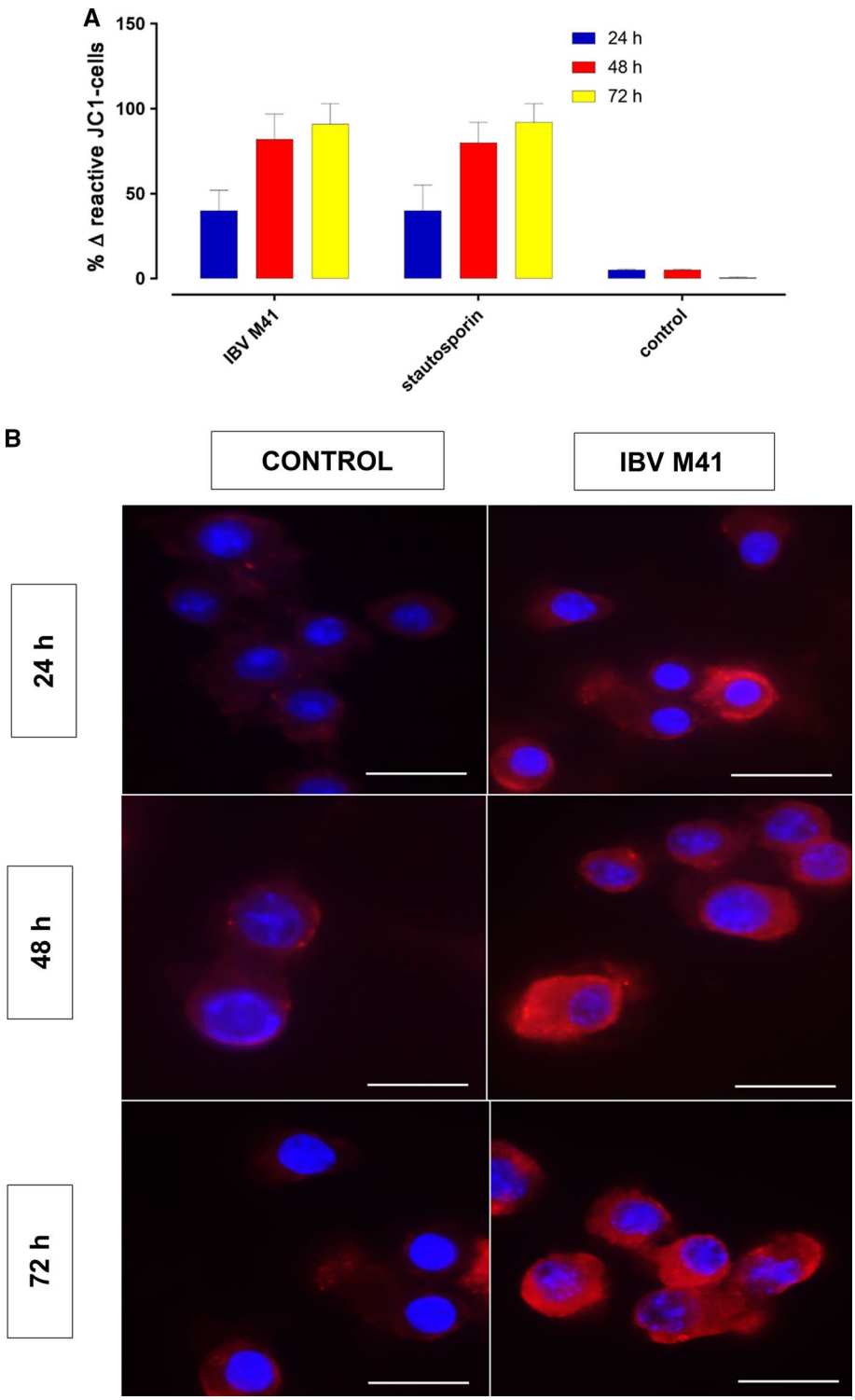

Fig. 2 A) Acoustic focusing cytometer analysis performed to measure JC-1 emission at all indicated times p.i. illustrated as % Δ of reactive cells in a bar graph. The data were obtained from three different experiments and processed using an Attune acoustic focusing cytometer with auto-fluorescence being excluded using a global compensation tool. B) JC-1 staining revealed red deposits in HD11 infected cells (bars 40-µm)

to activate the oxidative stress pathway to varying degrees (Fig. 3A). Mitochondrial oxygen consumption was monitored during IBV M41 infection and in mock infected cells (control). The parameters assessed were state-3 respiration (consumption of oxygen in the presence of respiratory substrate and ADP) and state-4 respiration (consumption of oxygen after ADP has been exhausted). After IBV M41 infection HD11 cells failed to undergo both state-3 and -4 respiration, when compared to mock infected cells (Fig. 3C). These results indicate that the IBV M41 strain acts as an uncoupler in the respiratory chain. One class of uncoupler is the protonophores, such as CCCP, which are weak acids

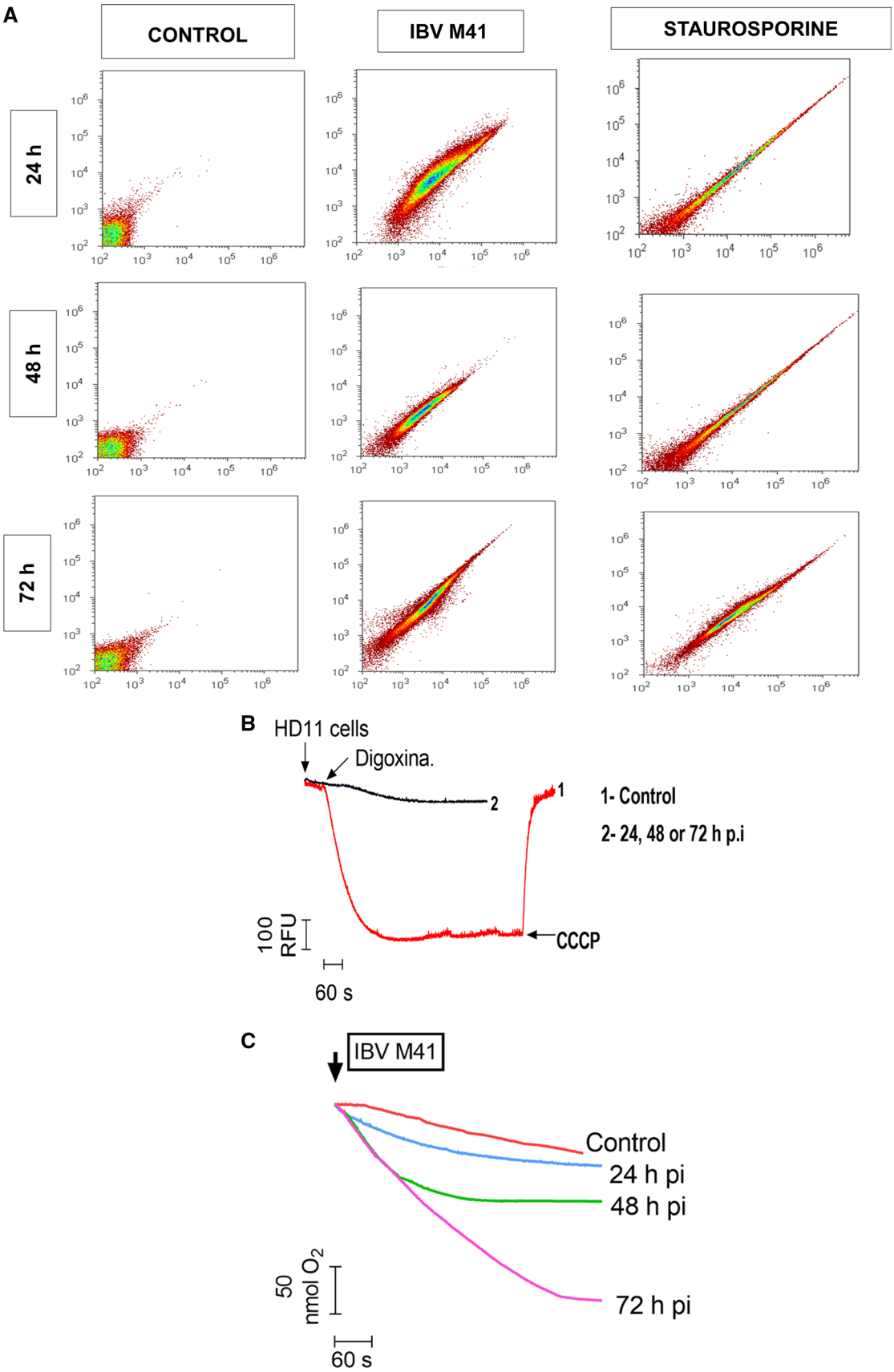
A
CONTROL
IBV M41
STAUROSPORINE
24 h
48 h
72 h
B
HD11 cells
Digoxina.
1
2
1- Control
2- 24, 48 or 72 h p.i
100 RFU
CCCP
60 s
C
IBV M41
Control
24 h pi
48 h pi
72 h pi
50 nmol O2
60 s

◂**Fig. 3** A) Detection of ROS production in HD11 cells infected with the IBV M41 strain, and respective controls, by flow cytometry analysis. These data are illustrated by density dot plot graphs where the x-axis corresponds to linear amplified ROS fluorescence and the y-axis indicates logarithmic ROS fluorescence. The fluorescence emission was acquired using a BL3A filter with auto-fluorescence being excluded using a global compensation tool ($> 10^3$), in a continuous line, using an Attune acoustic focusing cytometer. B) Effects of IBV M41 infection on mitochondrial membrane depolarization at 24, 48, and 72 h p.i. The presented microphotographs are representative images of three experiments. The arrows indicate the addition of compounds: C: control (macrophages without infection) or CCCP (1 μM of m-chlorophenyldrazone) acting as an uncoupler. C) Effects of IBV M41 infection on mitochondrial respiration at 24, 48 and 72 h p.i., showing a decrease in oxygen consumption

that increase the proton conductance of the inner mitochondrial membrane [19, 24]. IBV M41-infected macrophages demonstrated the capacity to induce ROS production at all examined times p.i., supporting the hypothesis that viral replication has a protonophoric activity in this study. During viral infection, macrophage functions may be directly compromised, affecting the immune system [22, 25]. This finding is of particular importance in poultry production, since an immunosuppressive state may lead to severe flock morbidity and mortality.

Taken together, our results indicate that IBV M41 infection acts as an uncoupler of oxidative phosphorylation, transforming the mitochondria from their normal role as an essential powerhouse in macrophage cells, and leading infected cells to undergo early apoptosis.

Acknowledgements The authors thank the Fundação de Amparo à Pesquisa do Estado de São Paulo (Grants 2012/16715-6) for their support. TC Cardoso is recipient of CNPq (Brazilian Council for Research) fellowships and funding.

Compliance with ethical standards

Funding Fundação Amparo à Pesquisa Estado de São Paulo (grant 2012/16715-6).

Ethical approval All applicable national (COBEA 2016/3456) for care and use animals were followed.

Conflict of interest All authors declare no conflicts of interests.

References

1. Amarasinghe A, Addul-Cader MS, Nazir S, De Silva Senapathi U, van der Meer F, Cork SC, Gomis S, Abdul-Careem F (2017) Infectious bronchitis coronavirus establishes productive infection in avian macrophages interfering with selected antimicrobial functions. PLoS One 12(8):e0181801
2. Awad F, Hutton S, Forrest A, Baylis M, Ganapathy K (2016) Heterologous live infectious bronchitis virus vaccination in day-old commercial broiler chicks: clinical signs, ciliary health, immune responses and protection against variant infectious bronchitis viruses. Avian Pathol 45:169–177
3. Barrow AD, Burgess SC, Baigent SJ, Howes K, Nair VK (2003) Infection of macrophages by a lymphotropic herpesvirus: a new tropism for Marek's disease virus. J Gen Virol 84:2635–2645
4. Brenner MPC, Silva-Frade C, Ferrarezi MC, Garcia AF, Flores EF, Cardoso TC (2012) Evaluation of developmental changes in bovine *in vitro* produced embryos following exposure to bovine Herpesvirus type 5. Rep Biol Endrocrinol 10:53
5. Cavanagh D (2007) Coronavirus avian Infectious bronchitis virus. Vet Rec 38:281–297
6. Chhabra R, Kuchipudi SV, Chantrey J, Ganapathy K (2016) Pathogenicity and tissue tropism of infectious bronchitis virus is associated and elevated apoptosis and innate immune responses. Virology 488:232–241
7. Clarke P, Tyler KL (2009) Apoptosis in animal models of virus-induced disease. Nat Rev Microbiol 7:144–155
8. Cook JK, Jackwood M, Jones RC (2012) The long view: 40 years of infectious bronchitis research. Avian Pathol 41:239–250
9. De Wit JJ (2000) Detection of infectious bronchitis virus. Avian Pathol 29:71–93
10. De Wit JJ, Cook JKA, van der Heijden HMJF (2011) Infectious bronchitis virus variants: a review of the history, current situation and control measures. Avian Pathol 40:223–235
11. Elmore S (2007) Apoptosis: a review of programmed cell death. Toxicol Pathol 35:495–516
12. Fung TS, Liu DX (2014) Coronavirus infection. ER stress, apoptosis and innate immunity. Front Microbiol 5:296
13. Geus ED, Verdelde L (2013) Regulation of macrophage and dendritic cell function by pathogens and through immunomodulation in the avian mucosa. Dev Comp Immunol 41:341–351
14. Han X, Tian Y, Guan R, Gao W, Yang X, Zhou L, Wang H (2017) Infectious bronchitis virus infection induces apoptosis during replication in chicken macrophage HD11 cells. Viruses 9(8):26
15. Jackwood MW (2012) Review of infectious bronchitis virus around the world. Avian Dis 56:634–641
16. Li FQ, Tam JP, Liu DX (2007) Cell cycle arrest and apoptosis induced by coronavirus infectious bronchitis virus in the absence of p53. Virology 365:435–445
17. Liu C, Xu HY, Liu DX (2001) Induction of caspase-dependent apoptosis in cultured cells by the avian coronavirus infectious bronchitis virus. J Virol 75:6402–6409
18. Maier H, Britton P (2012) Involvement of autophagy in coronavirus replication. Viruses 4:3440–3451
19. Nicotera P, Leist M, Ferrando-May E (1998) Intracellular ATP, a switch in the decision between apoptosis and necrosis. Toxicology 15:367–373
20. Ohta A, Nishiyama Y (2011) Mitochondria and viruses. Mitochondrion 11:1–12
21. Qureshi MA, Heggen CL, Hussain I (2000) Avian macrophage: effector functions in health and disease. Dev Comp Immunol 24:103–119
22. Iain Scott (2010) The role of mitochondria in the mammalian antiviral defense system. Mitochondrion 10:316–320
23. Skommer J, Brittain T, Raychaudhuri (2010) BcL-2 inhibits apoptosis by increasing the time-to-death and intrinsic cell-to-cell variation in the mitochondrial pathway of cell death. Apoptosis 15:1223–1233
24. Wallace KB, Starkov AA (2000) Mitochondrial targets of drug toxicity. Annu Rev Pharmacol Toxicol 40:353–388
25. West AP, Shadel GS, Ghosh S (2011) Mitochondria in innate immune responses. Nat Rev 11:389–402